

Immunopathology and Infectious Disease

YKL-40, a Marker of Simian Immunodeficiency Virus Encephalitis, Modulates the Biological Activity of Basic Fibroblast Growth Factor

Dafna Bonne-Barkay,* Stephanie J. Bissel,*
Gouji Wang,* Kenneth N. Fish,[†]
Georgina C.B. Nicholl,* Samuel W. Darko,*
Rafael Medina-Flores,* Michael Murphey-Corb,[‡]
Premeela A. Rajakumar,[‡] Julia Nyaundi,[‡]
John W. Mellors,[§] Robert Bowser,*
and Clayton A. Wiley*

From the Departments of Pathology,* Psychiatry,[†] Molecular
Genetics and Biochemistry,[‡] and Medicine,[§] University of
Pittsburgh, Pittsburgh, Pennsylvania

Human immunodeficiency virus encephalitis causes dementia in acquired immune deficiency syndrome patients. Using proteomic analysis of postmortem cerebrospinal fluid (CSF) and brain tissue from the simian immunodeficiency virus primate model, we demonstrate here a specific increase in YKL-40 that was tightly associated with lentiviral encephalitis. Longitudinal analysis of CSF from simian immunodeficiency virus-infected pigtailed macaques showed an increase in YKL-40 concentration 2 to 8 weeks before death from encephalitis. This increase in YKL-40 correlated with an increase in CSF viral load; it may therefore represent a biomarker for the development of encephalitis. Analysis of banked human CSF from human immunodeficiency virus-infected patients also demonstrated a correlation between YKL-40 concentration and CSF viral load. *In vitro* studies demonstrated increased YKL-40 expression and secretion by macrophages and microglia but not by neurons or astrocytes. We found that YKL40 displaced extracellular matrix-bound basic fibroblast growth factor (bFGF) as well as inhibited the mitogenic activity of both fibroblast growth factor receptor 1-expressing BaF3 cells and bFGF-induced axonal branching in hippocampal cultures. Taken together, these findings demonstrate that during lentiviral encephalitis, YKL-40 may interfere with the biological activity of bFGF and potentially of other heparin-binding growth factors and chemokines that can affect neuro-

nal function or survival. (Am J Pathol 2008, 173:130–143; DOI: 10.2353/ajpath.2008.080045)

Human immunodeficiency virus (HIV)-1-associated dementia [acquired immune deficiency syndrome (AIDS) dementia complex] is marked by deficits in motor control, cognition, and behavior.¹ At autopsy, AIDS patients with dementia exhibit neuropathological changes including infiltration of mononuclear cells as shown by abundance of perivascular macrophages and microglial nodules, glial cell activation, loss of synaptic integrity, and loss of select neuronal populations consistent with HIV encephalitis (HIVE).^{2,3} The pathogenesis of HIVE is not fully understood. One possible mechanism of neurodegeneration is that the neuroinflammatory cascade initiated by infiltrating monocytes disrupts the neuronal extracellular matrix (ECM) that normally provides physical support as well as a repository of growth and survival factors.⁴ To elucidate mechanisms leading to neurodegeneration in lentiviral encephalitis, we used mass spectrometry-based proteomics to identify proteins that are differentially expressed in the cerebrospinal fluid (CSF) of simian immunodeficiency virus (SIV)-infected macaques that do or do not develop encephalitis. Among the proteins that showed differential up-regulation in the CSF of SIVE cases was YKL-40. It is not known which cell types synthesize and release YKL-40 protein within the central

Supported by the National Institutes of Health (RO1 MH071151 and K24 MH01717 to C.A.W., and R21 MH073429 to C.A.W. and R.B.) and the Veterans Administration (Competitive Pilot Project Fund no. 02320).

D.B.-B. and S.J.B. contributed equally to this work.

Accepted for publication April 10, 2008.

Supplemental material for this article can be found on <http://ajp.amjpathol.org>.

Current address of S.J.B.: Department of Microbiology and Immunology, University of California Los Angeles, Los Angeles, CA; and R.M.-F.: Department of Pathology, University of New Mexico, Albuquerque, NM.

Address reprint requests to Clayton A. Wiley, M.D., Ph.D., Presbyterian University Hospital, Neuropathology Division, 200 Lothrop St., Pittsburgh, PA 15213. E-mail: claytonwiley@comcast.net.

nervous system (CNS) or what role YKL-40 may play in the neuropathogenesis of SIVE.

YKL-40 (HC-gp39, chitinase 3-like protein 1, CHI3L1, gp38k) is a member of the glycosyl hydrolase family 18 that lacks hydrolytic activity. From crystallographic analysis, YKL-40 has a carbohydrate-binding groove that can bind long or short oligosaccharides and it is speculated that it can also bind short chito-oligosaccharides used as primers for the synthesis of hyaluronic acid. Although YKL-40 contains a consensus motif for heparin binding, there is no conclusive evidence that heparin binds to this site. The less sulfated heparan sulfates are more likely to bind to the oligosaccharide-binding groove of YKL-40.⁵ Recently, YKL-40 was found to bind to types I, II, and III collagen in an interaction that required recognition of the collagen triple helix.⁶

YKL-40 is expressed and released by chondrocytes, synovial cells, neutrophils, and macrophages in late stages of differentiation. YKL-40 is up-regulated in inflamed tissue in ulcerative colitis, Crohn's disease, rheumatoid arthritis, osteoarthritis, scleroderma, and liver cirrhosis, as well as in cancers like melanoma, glioblastoma, and myeloid leukemia.^{7,8} The physiological role of YKL-40 is not clear, and the receptor through which it exerts its biological activity is not known. It has been shown to stimulate growth of chondrocytes, synoviocytes, and fibroblasts through activation of ERK and Akt signaling, promote adhesion and migration of vascular endothelial cells, increase proteoglycan synthesis in chondrocytes, inhibit cellular responses to tumor necrosis factor- α and interleukin (IL)-1 β in fibroblasts, and suppress the cytokine-induced secretion of matrix metalloproteinases 1, 3, and 13.⁹⁻¹²

Here, we report the identification of YKL-40 as a biomarker for SIVE. We show that YKL-40 is found in association with microglial nodules in SIVE and that it can bind to the ECM, modulating basic fibroblast growth factor (bFGF) biological activity.

Materials and Methods

Reagents

Purified YKL-40 was purchased from Quidel (San Diego, CA). Recombinant bFGF was purchased from R&D Systems (Minneapolis, MN) and iodinated bFGF was purchased from Perkin Elmer (Waltham, MA). Low-molecular weight heparin sodium salt from porcine intestinal mucosa and all other chemicals and media were purchased from Sigma (St. Louis, MO).

Animals

All animals were housed and maintained according to strict standards of the Association for Assessment and Accreditation of Laboratory Animal Care, and experiments were approved by the University of Pittsburgh Institutional Animal Care and Use Committee. Two groups of six and seven pigtailed macaques (*Macaca nemestrina*) varying in age from 74 to 93 months were intravenously infected with SIVDeltaB670 viral swarm

(SIVdB670).¹³ The length of infection varied from 42 to 287 days. Tissue samples from the first group of six macaques were available to measure YKL-40 before infection and at necropsy. Tissue samples from the second group of seven macaques were available to measure YKL-40 kinetics in CSF and plasma and compare them to viral load measurements. Plasma and CSF samples were drawn every 2 weeks. Macaques were sacrificed when moribund with AIDS or after 9 months of infection.

Quantitation of SIV and HIV RNA in CSF

Virions from 500 μ l of CSF were pelleted by centrifuging at 17,000 rpm for 1 hour. For SIV quantitation, total RNA was extracted from the virus pellet using Trizol (Invitrogen, Carlsbad, CA). Real-time reverse transcriptase-polymerase chain reaction (PCR) was performed with 20 μ l of each RNA sample as previously described.^{14,15} Primers and probes were specific for the SIV U5/LTR region. For HIV quantitation, HIV CSF quantitation was performed as previously described.¹⁶

Surface-Enhanced Laser Desorption/Ionization Time-of-Flight Mass Spectroscopy (SELDI-TOF-MS)

Strong anion exchange surface Q10 ProteinChips (Ciphergen Biosystems, Inc., Palo Alto, CA) were equilibrated with 100 mmol/L HEPES, pH 7.3 (titrated with NH₄OH). CSF samples from five SIVE macaques and three SIV without encephalitis macaques were first concentrated and desalted via C4 ZipTips (Millipore Corporation, Billerica, MA) and eluted onto the spots of the Q10 ProteinChip arrays using 70% acetonitrile and 0.1% trifluoroacetic acid. The arrays were incubated and washed in a ProteinChip bioprocessor (Ciphergen Biosystems, Inc.) and allowed to dry. A solution of sinapic acid (Fluka, Neu-Ulm, Germany) in 50% acetonitrile (ACN) and 0.3% trifluoroacetic acid was then added to each spot at 40°C. Spectra were acquired using the Ciphergen PBS IIC Chip Reader (Ciphergen Biosystems, Inc.). Low-mass (2 to 20 kDa) time-of-flight spectra were generated by averaging 195 ionizations per spot with a laser intensity of 175 and a detector sensitivity of 7, and high mass (20 to 160 kDa) spectra were acquired by using a laser intensity of 182 and a detector sensitivity of 8. The spectra were calibrated using All-in-1 protein standard (Ciphergen Biosystems, Inc.). Spectra were normalized using total ion current, baseline subtraction, and a normalization coefficient of 0.2. CSF samples were analyzed in duplicate within each experiment, and a standard CSF sample was used on each separate array to control for variability between chips. All experiments were performed three times. Univariate analysis was performed using the clustering feature of the ProteinChip software (Ciphergen Biosystems, Inc.).

Protein Identification by Mass Spectrometry

For anion exchange fractionation, pooled CSF (500 μ l) was diluted with 1 mol/L Tris-HCl at pH 9.0 and then added by gravity flow to a Micro Bio-Spin chromatography column (Bio-Rad, Hercules, CA) that had been equilibrated with 50 mmol/L Tris-HCl at pH 9.0 and loaded with a slurry of Q HyperD F matrix (Ciphergen Biosystems). Fractions were collected with buffers containing 0.1% OGP detergent at varying pH: pH 9.0 (20 mmol/L Tris-HCl), pH 7.0 (50 mmol/L HEPES), pH 5.0 (100 mmol/L sodium acetate), pH 4.0 (100 mmol/L sodium acetate), and pH 3.0 (50 mmol/L sodium citrate). The column was then washed with 33% isopropanol, 17% ACN, and 0.1% trifluoroacetic acid to collect any proteins not eluted by pH. To determine which fraction contains the protein peak of interest, 2 μ l of each fraction was applied to both Q10 and NP20 ProteinChip arrays (Ciphergen Biosystems) and analyzed by SELDI-TOF-MS for the presence of the 38.2-kDa peak present in SIVE animals.

To determine the protein identity of the 38.2-kDa mass peak, proteins from the appropriate column fractions were separated by sodium dodecyl sulfate-polyacrylamide gel electrophoresis. Gel slices at \sim 38 kDa were washed with NH_4HCO_3 and 50% ACN and dried in a speed vacuum. The gel pieces were incubated with 10 mmol/L dithiothreitol in 25 mmol/L NH_4HCO_3 at 56°C for 1 hour followed by 55 mmol/L iodoacetamide in 25 mmol/L NH_4HCO_3 at room temperature for 45 minutes in the dark. To dehydrate the protein, pellets were washed with 50 mmol/L NH_4HCO_3 followed by 25 mmol/L NH_4HCO_3 in 50% ACN and dried in a speed vacuum. The protein was rehydrated with 12.5 ng/ μ l sequence grade trypsin (Promega, Madison, WI) in 25 mmol/L NH_4HCO_3 for 10 minutes on ice and incubated at 37°C overnight. The aqueous phase was transferred into a clean siliconized tube, and the pellet was agitated with 50% ACN and 5% formic acid for 20 to 30 minutes. The supernatant was dried in a speed vacuum and resuspended in 50% high performance liquid chromatography-grade $\text{H}_2\text{O}/50\%$ ACN/0.3% trifluoroacetic acid containing 4-hydroxy- α -cinnamic acid. Tryptic digests were applied for peptide sequencing using an Applied Biosystems 4700 proteomics analyzer (Applied Biosystems Inc., Foster City, CA). Peptide amino acid sequences were compared with Mascot protein databases with a peptide mass tolerance of ± 50 ppm to confirm protein identity.

YKL-40 Enzyme-Lined Immunosorbent Assay (ELISA)

YKL-40 levels were determined, in duplicate, for all of the CSF samples using the Metra YKL-40 ELISA kit from Quidel according to the manufacturer's protocol. Absorbance was measured using a microplate reader (Beckman Coulter, Fullerton, CA).

Protein Extraction from Brain Tissue and Immunoblotting

Protein was extracted from 100 mg of middle frontal cortex as described previously.¹⁷ In brief, samples were homogenized in extraction buffer (25 mmol/L Hepes, 50 mmol/L NaCl, 5 mmol/L ethylenediaminetetraacetic acid, pH 7.5) containing 10 μ l/ml of Halt protease inhibitor cocktail (Pierce Biotechnology, Inc., Rockford, IL) using a Tissue-Tearor homogenizer (Biospec Products, Inc., Bartlesville, OK). Tissue extracts were centrifuged (two times), supernatants collected, and protein quantified using Coomassie Plus protein assay reagent (Pierce). For immunoblot analysis, 50 μ g of protein from each sample was separated on 16% Novex Tris-glycine gels (Invitrogen), transferred to polyvinylidene difluoride membranes (Bio-Rad Laboratories), blocked with 5% milk or bovine serum albumin (Fisher Scientific, Pittsburgh, PA) in phosphate-buffered saline (PBS) containing Tween 20 (Bio-Rad), and then incubated with either anti-human chitinase 3-like 1 (goat polyclonal, 1:50; R&D Systems) or anti- β -actin (mouse monoclonal, 1:5000; Abcam, Cambridge, MA). Membranes were washed and incubated with species-specific secondary antibodies tagged with horseradish peroxidase (Pierce). A signal was visualized with a SuperSignal West Pico chemiluminescent substrate system (Pierce).

Primary Cell Cultures

Macrophage cultures were obtained from human peripheral blood mononuclear cells isolated from HIV and hepatitis B sero-negative buffy coats obtained from the Central Blood Bank (Pittsburgh, PA) using Cellgro lymphocyte separation medium (Mediatech Inc., Herndon, VA).¹⁸ CD14-positive cells were isolated by positive selection with magnetic beads conjugated to anti-CD14 (Miltenyi Biotech, Auburn, CA). Isolated monocytes were cultured in plates coated with poly-D-lysine (20 μ g/ml) with the presence of M-CSF (100 ng/ml) for 7 days. More than 95% of the cells were macrophages and stained for CD68. Primary human embryonic mixed glial-neuronal cultures were obtained from human fetal tissue collected as per standards of the University of Pittsburgh ethics and biosafety guidelines and established protocols.¹⁹ In brief, brain tissues from week 18 embryos were incubated with trypsin-ethylenediaminetetraacetic acid for 45 minutes. The tissue was triturated with a 10-ml pipette followed by a 5-ml pipette and then passed through 100 μ m, 70 μ m, and 40 μ m meshes. The cells were cultured on Permax chamber slides coated with 20 μ g/ml of poly-D-lysine or in flasks with Dulbecco's modified Eagle's medium/F12 supplemented with 10% FBS (HyClone, Logan, UT). Microglia were separated from the mixed glial-neuronal cultures by shaking the cultures on an orbital shaker and collecting the detached cells. Purified astrocyte cultures were obtained by trypsinization of the mixed glial-neuronal cultures followed by two passages.

Dissociated Primary Hippocampal Cultures

Neurons were cultured at low density from embryonic day 18 (E18) Sprague Dawley rat hippocampi, as previously described.²⁰ After 2 days in culture the cultures were transferred from the feeder layer and grown in serum-free N2.1 medium in the absence or presence of bFGF, heparin, and YKL-40.

Immunohistochemistry

Formalin-fixed, paraffin-embedded sections were deparaffinized in HistoClear (National Diagnostics, Atlanta, GA) and rehydrated for 3 minutes in 100%, 95%, and 70% alcohol followed by PBS. Endogenous peroxidase activity was inactivated by immersing the section in 3% H₂O₂ for 20 minutes. Antigen unmasking was performed using antigen retrieval citra solution (BioGenex, San Ramon, CA). Tissue sections were blocked with protein blocking agent (Thermo, Pittsburgh, PA) for 20 minutes. Tissue cultures were fixed with 4% paraformaldehyde and sucrose for 20 minutes. YKL-40 staining was performed using goat anti-human chitinase 3-like antibody (1:1000, R&D Systems) as primary antibody followed by mouse anti-goat biotin-conjugated antibody (1:200; Jackson ImmunoResearch Laboratories, West Grove, PA) and detected by the tyramide amplification system (Perkin Elmer Life Sciences, Boston, MA). For double-label immunofluorescent antibodies: polyclonal rabbit anti-human GFAP (1:500; DAKO, Carpinteria, CA), monoclonal mouse anti-human MAP2 (1:1000; Sternberger Monoclonals, Inc., Lutherville, MD), and monoclonal mouse anti-human CD68 (1:100, DAKO) were used at stated dilutions without amplification. Dissociated primary hippocampal cultures were stained with monoclonal anti- β -tubulin isotype III (Sigma). All of the secondary antibodies were used from Jackson Laboratories (Bar Harbor, ME). Slides were mounted in gelvatol and analyzed by laser confocal microscopy (Carl Zeiss MicroImaging, Inc., Thornwood, NY).

Dual in Situ Hybridization and Immunohistochemistry

Antisense YKL-40 DNA templates containing the T7 promoter were generated by RT-PCR from cDNA prepared from primary pigtailed macaque primary macrophage culture. Two probes were made from different regions of the cDNA one corresponding to bases 19 to 241, forward primer, 5'-TTATACGACTCACTATAGGGAGAAAACAGGCTTTGTGGTCCTG-3'; reverse primer, 3'-CTGTGAGATGCCGTACGAGT-5'. The second probe was corresponding to bases 429 to 673, forward primer, 5'-TTATACGACTCACTATAGGGAGAACGGAGAGACAAGCAGCATT-3'; reverse primer, 3'-AGTATCAGGGGACAAGGCTC-5'. Sense probes were made by adding the T7 promoter sequence to the reverse primers. ³⁵S-labeled RNA probes were generated using MAXIscript kit (Ambion, Austin, TX). Sections from SIVE cases in paraffin blocks were cut into serial sections of 6 μ m, deparaffinated, and

processed for immunohistochemistry and then to *in situ* hybridization as described previously.²¹

Preparation of Dishes Coated with ECM

Bovine corneal endothelial cells (American Type Culture Collection, Manassas, VA) were maintained in high-glucose Dulbecco's modified Eagle's medium supplemented with 10% fetal bovine serum. For ECM preparation, the cells were plated at a density of 5000 cells per well in a 96-well plate in growth medium supplemented with 5% dextran. When the culture reached confluency, the cells were lysed with a solution containing 0.5% Triton X-100, 20 mmol/L NH₄OH in PBS for 3 minutes at room temperature followed by four washes with PBS.²²

YKL-40 Displacement of ECM-Bound ¹²⁵I-bFGF

ECM was incubated with iodinated bFGF (80,000 cpm/well, 3 hours, room temperature) in RPMI medium containing 0.2% gelatin, and unbound bFGF was removed by four washes with PBS containing 0.02% gelatin. The ECM was then incubated (3 hours, 37°C, PBS containing 0.02% gelatin) with increasing concentrations of heparin, bovine serum albumin, or YKL-40. Aliquots (0.25 ml) of the incubation medium were counted in a γ -counter to determine the amount of released iodinated material. The remaining ECM was washed twice. The percentage of released ¹²⁵I-bFGF was calculated from the total ECM-associated radioactivity, solubilized with 1 mol/L NaOH, and counted in a γ -counter.²²

FGFR1-Expressing Baf3 Cell Culture and Mitogenic Assay

Suspension cultures of FGFR1a (IIIc)-expressing BaF3 cells (a generous gift from professor D.M. Ornitz, Washington University, St. Louis, MO) were maintained in RPMI 1640 medium (Sigma) supplemented with 10% newborn calf serum (Sigma), 0.5 ng/ml murine recombinant IL-3 (Peprotech, Rocky Hill, NJ), 2 mmol/L L-glutamine, penicillin-streptomycin, 50 nmol/L β -mercaptoethanol, and G418 (600 μ g/ml).²³

For the mitogenic assay, the cells were washed three times with PBS and plated at a density of 30,000 cells per well in a 96-well plate in growth medium without IL-3 with the absence or presence of 5 ng/ml bFGF, 1 μ g/ml heparan sulfate, and varying concentrations of YKL-40 for 48 hours. Heparan sulfate and YKL-40 were mixed and incubated on ice for 1 hour before their addition. Proliferation of the cells was evaluated using Promega's CellTiter kit.²⁴

Morphological Analysis

Cells (14 to 48) bearing neurites were selected randomly in each group. Images were collected on an Olympus IX-81 microscope (Olympus America Inc., Melville, NY) equipped with a Hamamatsu C4742-98 charge-coupled device camera (Hamamatsu Corporation, Bridgewater,

NJ) and a Ludl motorized XYZ stage (LEP Ltd., Hawthorne, NY). To quantify axonal characteristic five sequential slices taken 0.5 μm apart through the midplane of the axon were collected with a U plan S Apo 20 \times 0.75 N.A. objective using SlideBook 4.1 Imaging software (Intelligent Imaging Innovations, Inc., Denver, CO). A projection image was made of the image stack and the reconstructed images were then delineated and the threshold set. The number of axonal branch points per neuron counted. Importantly, the person counting the branch points was blind to the treatment conditions.

Statistical Analyses

A one-way analysis of variance with posthoc comparison via Tukey's honestly significant difference was used to evaluate between group differences. In all cases, diagnostic statistics were used to confirm that the data were normally distributed.

Results

Proteomic Mass Spectrometric Analysis Identifies Increased YKL-40 in CSF of Macaques with SIVE

In the past few years, researchers have used proteomic analyses of CSF to discover specific biomarkers in neurological diseases such as amyotrophic lateral sclerosis,²⁵ multiple sclerosis,²⁶ Alzheimer's disease,²⁷⁻²⁹ or primary brain tumors.³⁰ Such biomarker discovery studies may reveal biochemical or cellular processes involved in the neurodegenerative disease, and proteins that may represent biomarkers for that disease. This information would be useful because diagnosing chronic encephalitis induced by lentiviruses in human and non-human macaques is particularly complicated by the subtlety of early neurological signs and symptoms and the potential for systemic immune compromise to manifest neurological findings.

Recent studies examining CSF or monocyte-derived macrophages from HIV-infected patients have found spectral peak differences between demented and non-demented individuals.³¹⁻³³ However, these reports did not determine the protein identities of the mass peaks of interest. To discover additional proteins that may participate in the pathogenesis of HIV/SIV-induced encephalitis, we performed mass spectrometry-based proteomics of CSF samples from SIV-infected macaques with and without encephalitis using SELDI-TOF-MS. We identified 4 spectral peaks that were exclusive to macaques with encephalitis, 4 spectral peaks exclusive to macaques without encephalitis, and 14 spectral peaks that were increased or decreased in macaques with encephalitis compared with nonencephalitic controls. One mass peak of ~ 38.2 kDa exhibited an approximate fivefold elevation in relative peak intensity in SIVE versus SIV without encephalitis (Figure 1). We enriched for this mass peak by ion

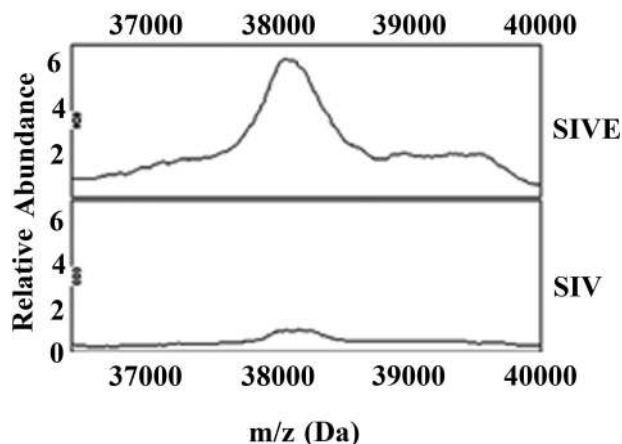


Figure 1. Comparison of mass spectra from CSF between SIV-infected macaques with and without encephalitis using Q10 ProteinChips shows differences in signal intensities of protein peaks. Representative spectral peaks of SIV-infected macaque with encephalitis (SIVE) (**top**) and SIV-infected macaque without encephalitis (SIV) (**bottom**). The *x* axis shows the mass-to-charge (*m/z*) ratio in Da (36,000 to 40,000 Da), and the *y* axis shows the relative abundance (peak intensities). A mass peak of 38,200 Da was evident at significantly increased levels in SIVE macaques.

exchange chromatography and then determined its protein identity by tryptic digestion and tandem mass spectrometry (see Materials and Methods). Fifteen peptide fragments representing this mass peak were identified as YKL-40 using the MASCOT search engine, providing 44% sequence coverage for this protein and a Mowse probability score of 79 (data not shown). To validate the mass spectrometry results, we performed both Western blot (Figure 2A) and ELISA analysis (Figure 2B) of brain tissue and CSF from SIVE, SIV without encephalitis, and noninfected control animals using antibodies specific to YKL-40. These results confirm the increased levels of YKL-40 protein in the CSF and brain tissue of SIVE macaques.

YKL-40 Levels in the CSF of SIV-Infected Pigtailed Macaques Correlates with the CSF Viral Load and the Development of Encephalitis

Because we identified YKL-40 as differentially up-regulated in CSF of necropsied macaques with SIVE, it was of interest to determine the kinetics of YKL-40 in the CSF of SIV-infected macaques especially because YKL-40 has been reported to be elevated in inflammatory conditions such as rheumatoid arthritis and osteoarthritis and acute infectious conditions such as purulent meningitis and pneumococcal bacteremia.^{34,35} A second group of seven macaques were challenged with SIVDeltaB670 viral swarm, and plasma and CSF samples were drawn every 2 weeks. CSF and plasma YKL-40 concentrations were analyzed by ELISA and compared with the pathological findings at necropsy. Noninfected macaques have an average CSF concentration of 144 ng/ml YKL-40 (range, 66.2 to 222 ng/ml). Longitudinal analysis of YKL-40 concentrations during the course of SIV infection shows initially low levels of CSF YKL-40 (range, 204 to 365 ng/ml) followed by a rapid rise 2 to 8 weeks before death in animals that show SIV encephalitis at necropsy

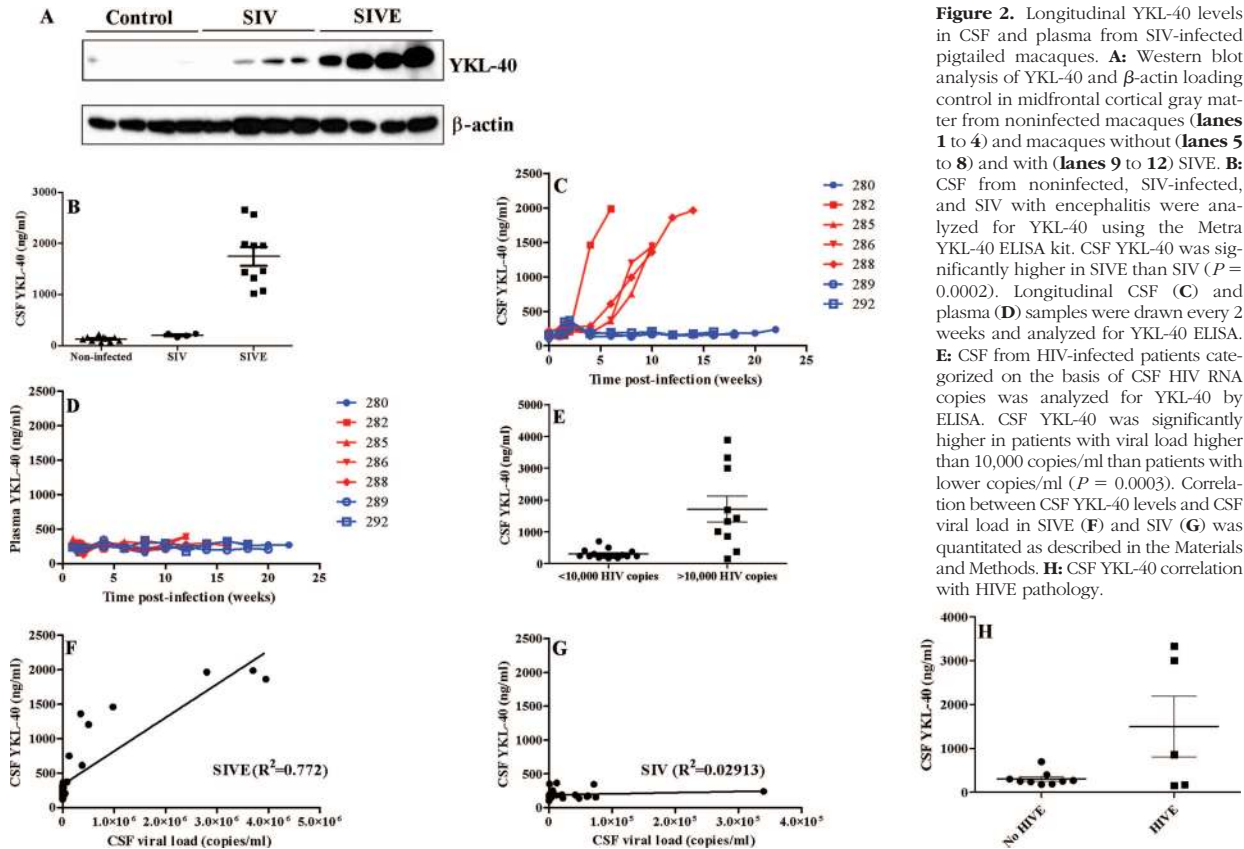


Figure 2. Longitudinal YKL-40 levels in CSF and plasma from SIV-infected pigtailed macaques. **A:** Western blot analysis of YKL-40 and β -actin loading control in midfrontal cortical gray matter from noninfected macaques (**lanes 1 to 4**) and macaques without (**lanes 5 to 8**) and with (**lanes 9 to 12**) SIVE. **B:** CSF from noninfected, SIV-infected, and SIV with encephalitis were analyzed for YKL-40 using the Metra YKL-40 ELISA kit. CSF YKL-40 was significantly higher in SIVE than SIV ($P = 0.0002$). Longitudinal CSF (**C**) and plasma (**D**) samples were drawn every 2 weeks and analyzed for YKL-40 ELISA. **E:** CSF from HIV-infected patients categorized on the basis of CSF HIV RNA copies was analyzed for YKL-40 by ELISA. CSF YKL-40 was significantly higher in patients with viral load higher than 10,000 copies/ml than patients with lower copies/ml ($P = 0.0003$). Correlation between CSF YKL-40 levels and CSF viral load in SIVE (**F**) and SIV (**G**) was quantitated as described in the Materials and Methods. **H:** CSF YKL-40 correlation with HIVE pathology.

(Figure 2C). At necropsy the encephalitic animals showed elevated YKL-40 levels (median, 1465 ng/ml; range, 1026 to 2662 ng/ml), whereas nonencephalitic macaques had a median level of 215 ng/ml (range, 166 to 238 ng/ml) (Figure 2B). The increase in YKL-40 concentration more than 500 ng/ml in the CSF preceded their death from 2 to 8 weeks. Plasma YKL-40 levels do not change throughout the course of infection indicating that YKL-40 is specifically increased in the CNS and not a general systemic phenomenon of infection (Figure 2D). Similar results were obtained in CSF from HIV patients. YKL-40 was higher in patients with HIV viral load higher than 10,000 copies/ml (median, 1382 ng/ml; range, 156 to 3894 ng/ml) (Figure 2E) and there was a significant elevation in CSF YKL-40 in HIV patients with HIVE versus patients without encephalitis (Figure 2H). Within animals that developed encephalitis, YKL-40 concentrations correlated with SIV CSF viral load (R^2 value range = 0.7825 to 0.9698) (Table 1). The pooled analysis from four encephalitis macaques also showed a correlation between YKL-40 levels and CSF viral load ($R^2 = 0.772$) (Figure 2F) as opposed to the three nonencephalitic animals ($R^2 = 0.1296$) (Figure 2G).

In Vitro YKL-40 Is Expressed in Microglia but Not Astrocytes and Neurons

YKL-40 is released from a variety of cells *in vitro*, including chondrocytes and synoviocytes isolated from rheumatoid arthritis patients, vascular smooth muscle cells,

macrophages in late stage of differentiation, activated macrophages and neutrophils, as well as cancer cell lines such as the osteosarcoma MG63. *In vivo*, YKL-40 is released from macrophages and vascular smooth muscle cells in atherosclerotic plaques, macrophages in inflamed synovial membranes, and peritumoral macrophages in small cell lung cancer, and is expressed in many types of solid tumors.³⁶ We are not aware of previous publications describing YKL-40 expression in cell types of the CNS. To determine the cell types in the CNS that express YKL-40, we used primary human fetal brain cultures of mixed glial-neuronal cultures as well as isolated astrocyte and microglia cultures stained with an antibody against human YKL-40. As shown in Figure 3,

Table 1. CSF YKL-40 and Viral Load Correlates with SIVE but Not SIV

Animal no.	Pathology	YKL-40/viral load correlation (R^2)	Pooled YKL-40/viral load correlation (R^2)
280	SIV	0.1746	0.02913
289	SIV	0.0312	
292	SIV	0.4919	
282	SIVE	0.8357	0.772
285	SIVE	0.9146	
286	SIVE	0.9698	
288	SIVE	0.7825	

CSF YKL-40 and viral load of the encephalitic animals 282, 285, 286, and 288 were combined to create a pooled correlation with a correlation coefficient of $R^2 = 0.02913$. The nonencephalitic animals 280, 289, and 292 have a correlation coefficient of $R^2 = 0.772$.

YKL-40 co-localizes with the microglia/macrophage marker CD68, and not in neurons or astrocytes denoted by MAP2 or GFAP, respectively. Because YKL-40 is a released protein, we further confirmed the results by measuring YKL-40 levels in the culture medium. Primary human macrophage cultures were used as positive controls. Primary microglia cultures express and secrete low levels of YKL-40 into the culture medium; however, treatment with lipopolysaccharide does not induce changes in secretion (Figures 4 and 5). Cultured astrocytes do not express or secrete YKL-40, nor do they secrete YKL-40 when activated with DBcAMP (Figure 4).

In Vivo YKL-40 Is Deposited Around Astrocytes in the Vicinity of Microglial Nodules in SIVE and HIVE

To determine the cellular distribution of YKL-40 in the CNS, tissue sections from encephalitic monkeys and HIVE patients were immunostained with antibodies against YKL-40, CD68, and GFAP. As shown in Figures 6 and 7, YKL-40 staining was found surrounding astrocytes in the vicinity of microglial nodules and in the cytoplasm of perivascular macrophages. Surprisingly, YKL-40 was distributed as a cloud around activated astrocyte cell bodies (Figure 8; and supplemental movie, see <http://ajp.amjpathol.org>). YKL-40 staining was not detected in the macrophages in the nodules. To determine the cellular source of YKL-40 we performed *in situ* hybridization. Figure 9 shows that YKL-40 mRNA co-localizes with CD68 staining, indicating that microglia/macrophages are the main source of YKL-40.

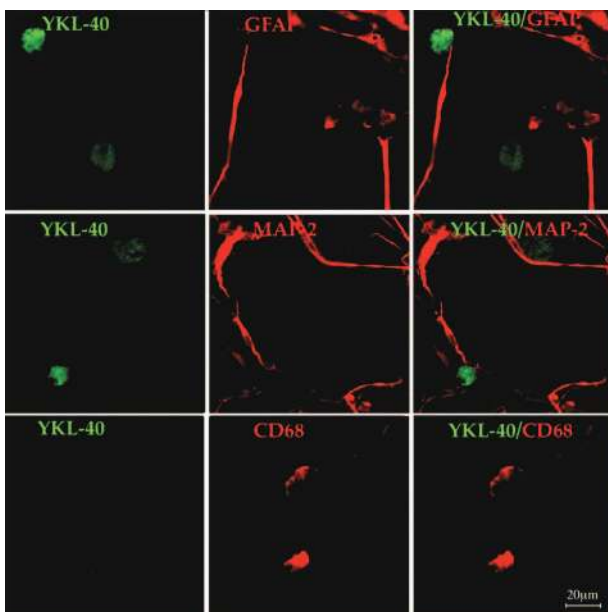


Figure 3. YKL-40 stain co-localizes with macrophage/microglial marker. Mixed glia-neuronal cultures were prepared as described in the Materials and Methods. On day *in vitro* (DIV) 4 the cultures were double-labeled for YKL-40 (green) and MAP2 (red) or GFAP (red) or CD68 (red).

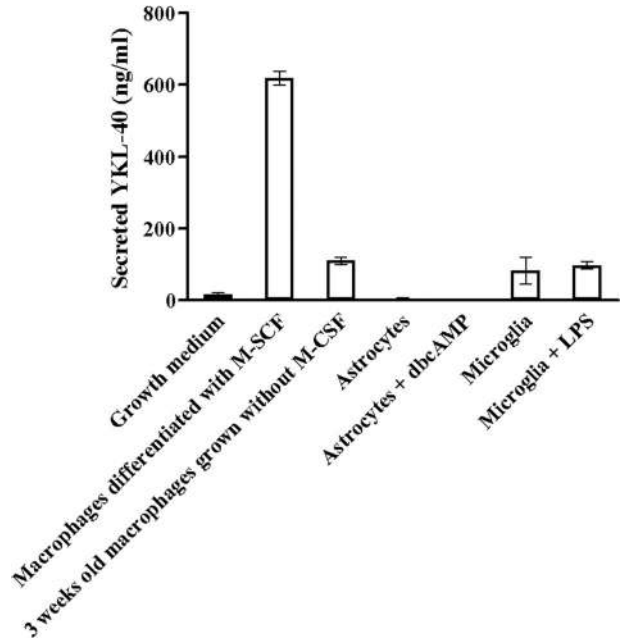


Figure 4. YKL-40 is secreted from human primary microglia and macrophages but not astrocyte cultures. Human primary microglia, astrocyte, and macrophage cultures were prepared as described in the Materials and Methods. YKL-40 secretion into the culture medium was measured 4 days after plating using the Metra YKL-40 ELISA kit or 2 weeks after excluding M-CSF from the media for macrophages. One µg/ml of LPS and 1 mmol/L dibutylryl cyclic adenosine monophosphate (DBcAMP) were added to microglia or astrocyte cultures, respectively, 48 hours before assay performance.

YKL-40 Induces bFGF Release from ECM and Inhibition of bFGF-Induced Proliferation of FGFR1c-Expressing BaF3 Cells as Well as bFGF-Induced Axonal Branching

Crystallographic studies suggest that YKL-40 has a putative heparin/heparan sulfate binding domain and therefore may interact with glycosaminoglycan chains on proteoglycans deposited in the matrix or on the cell surface.⁵ Heparan sulfate proteoglycans can modulate the activities of FGFs, cytokines, and chemokines by immobilizing or protecting them from proteolysis or regulating their receptor dimerization and subsequent signaling.^{37,38} bFGF has been studied

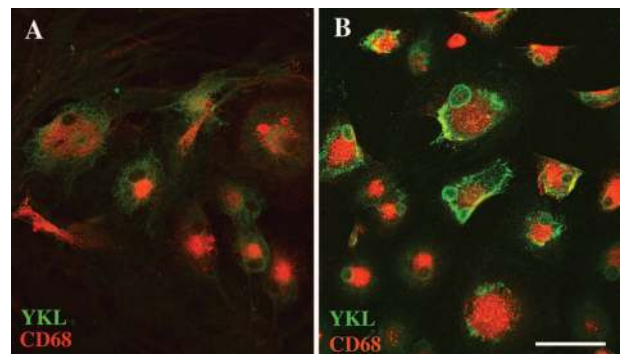


Figure 5. YKL-40 macrophage staining in human primary cultures and microglia. Human primary microglia and macrophage cultures were prepared as described in the Materials and Methods. On DIV 4 the cultures were double-labeled with YKL-40 (green) and CD68 (red). Scale bar = 50 µm.

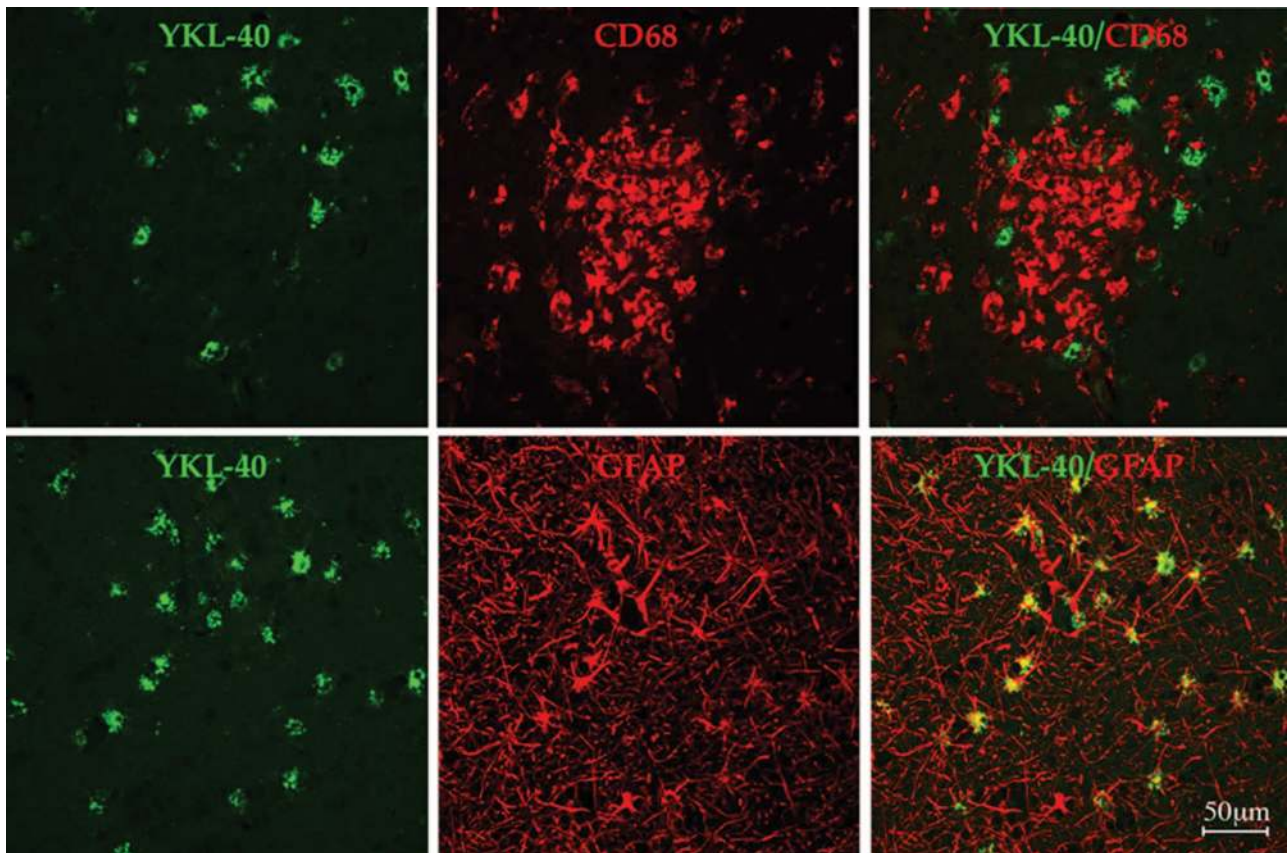


Figure 6. YKL-40 localizes around astrocytes in regions of microglial nodules in SIVE. Double-label immunofluorescence for YKL-40 (green) and CD68 (red) or GFAP (red). Co-localization of YKL around GFAP-positive astrocytes is evident in the yellow signal around cell bodies.

extensively and therefore used as a model to test the hypothesis that YKL-40 through its heparin binding domain can displace ECM-bound growth factors from their ECM binding sites and also interfere with biological activities induced by this growth factor. As shown in Figure 10, YKL-40 can displace ECM-bound bFGF, although not as efficiently as heparin, suggesting that YKL-40 can bind to a subset of bFGF-ECM binding sites. It was previously shown that bFGF can induce mitogenic activity in FGFR1-expressing Baf3 cells only in the presence of heparin/heparan sulfate. Addition of YKL-40 inhibited the mitogenic activity induced by bFGF in a dose-dependent manner (Figure 11). YKL-40 and heparan sulfate by themselves do not induce any mitogenic activity in these cells. Previous reports show that bFGF promotes survival, enhances neurite extension and axonal branching in primary neuronal cultures.³⁹⁻⁴⁴ Using dissociated hippocampal neuronal cultures we have assessed the role of YKL-40 to inhibit the trophic effects of bFGF. Figure 12 shows a qualitative and quantitative assessment of these cultures demonstrating a significant effect of YKL-40 on inhibiting the sprouting of axonal branches.

Discussion

In this study we found that YKL-40 is elevated in the CSF of pigtailed macaques infected with SIV that develop encephalitis and that there is a correlation between the CSF viral

load and YKL-40 levels. YKL-40 was expressed in microglia/macrophages but not astrocytes and neurons *in vitro*. The differentiation protocol of monocytes contains M-CSF that could account for induced YKL-40 levels as opposed to previously differentiated microglia cultured without M-CSF. Washing the M-CSF and growing the culture for an additional 2 weeks resulted in lower monocyte-derived macrophage release of YKL-40 into the culture media to levels equivalent to microglia (Figure 4). *In vivo* YKL-40 is predominantly associated with astrocytes in the vicinity of microglial nodules. Initial characterization of the biological role of YKL-40 shows that YKL-40 can bind to the ECM and is capable of displacing ECM-bound bFGF as well as blocking biological activities of this growth factor in neurons.

YKL-40 as a CSF-Specific Biomarker of SIV Encephalitis

Ostergaard and colleagues (2002) previously reported higher YKL-40 levels in the CSF of patients with purulent meningitis or encephalitis than in patients with or without lymphocytic meningitis.³⁵ In agreement with these findings, our longitudinal analysis of CSF of SIV-infected monkeys showed that YKL-40 levels increased between 2 to 8 weeks before death and were found to be 10-fold higher in the CSF than in the plasma. Therefore YKL-40 may serve as a CSF biomarker for the development of encephalitis. Previous studies have shown that high viral

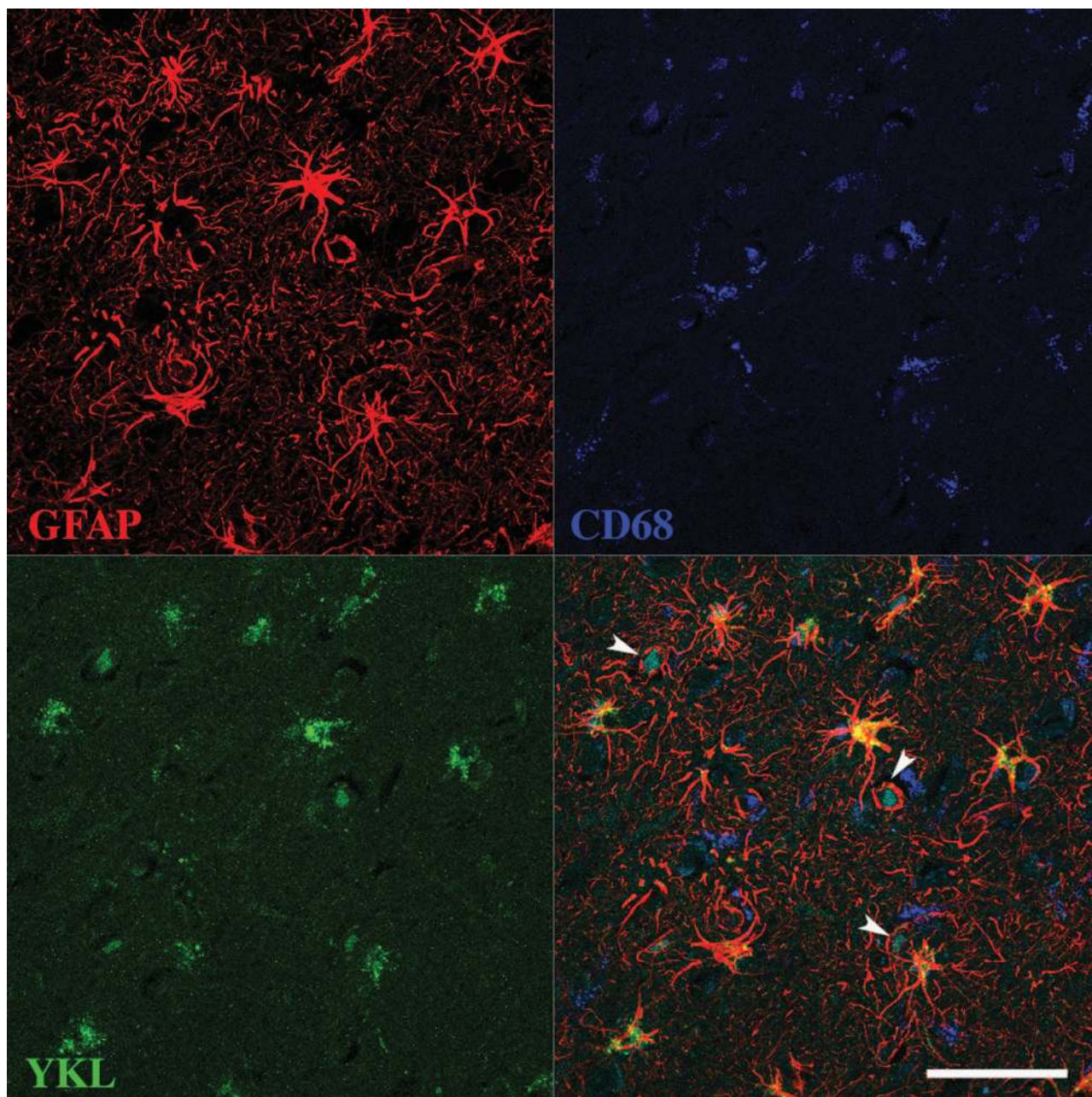


Figure 7. YKL-40 localizes around astrocytes in regions of microglial nodules and occasional CNS activated macrophages/microglia in HIV-1. Triple-label immunofluorescence for YKL-40 (green) and CD68 (blue) or GFAP (red). Co-localization of YKL-40 and astrocytes appears as yellow halo around cell soma. Co-localization of YKL with CD68-positive macrophages is evident by aqua signal (**arrowheads**). Scale bar = 50 μ m.

load in the CSF correlates with severity of SIV encephalitis^{45,46} and in humans high HIV load in the CSF correlated with presence of HIV encephalitis at autopsy.^{16,47} Our study has shown that YKL-40 levels in SIVE correlated with CSF viral load, which further supports its potential use as a biomarker of SIVE.

Other CSF Biomarkers of SIV Infection

Other molecules such as IL-6, MCP-1, 14-3-3, quinolinic acid, prostaglandin D2, platelet-activating factor, Fas, and Fas ligand, and the light subunit of neurofilament protein

have been suggested as predictors of CNS disease.^{48–52} Most of these markers have been analyzed in human cross-sectional rather than longitudinal studies. Previous longitudinal CSF studies in SIV encephalitis have shown elevation of IL-6 and MCP-1. CSF IL-6 levels were persistently elevated beginning at 4 weeks after infection, peaking at 8 weeks after infection, and then declining gradually thereafter. Infected macaques also had elevated levels of MCP-1 both in the CSF and plasma at 10 days after infection after which MCP-1 levels declined. In macaques that developed moderate to severe encephalitis, CSF MCP-1 levels increased again at 28 days after infection and continued to increase

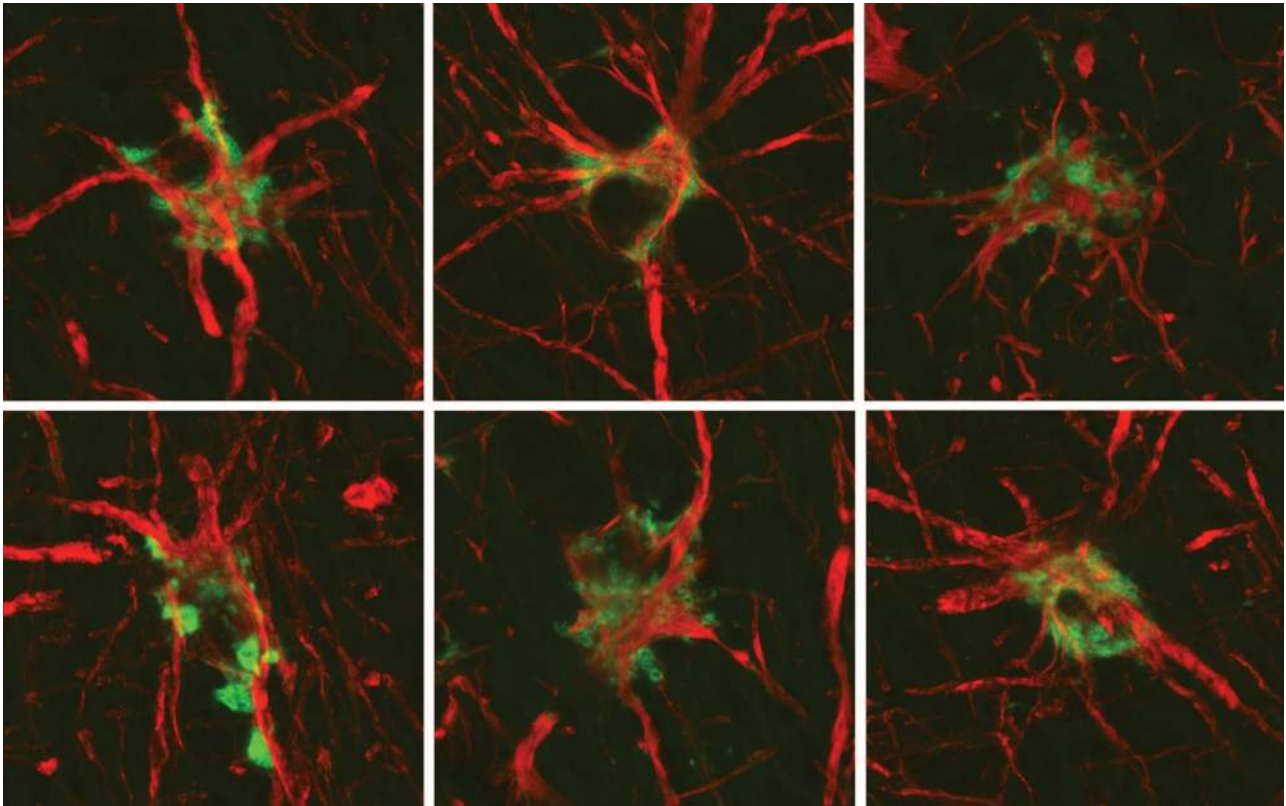


Figure 8. YKL-40 is distributed around activated astrocyte cell bodies in regions with microglial nodules. Six different astrocytes double-label for YKL-40 (green) and GFAP (red). See Supplemental Movie at <http://ajp.amjpathol.org> for the spatial deposition of YKL-40 around the astrocyte soma.

throughout the remainder of infection. In contrast macaques that had no or mild encephalitis had low CSF MCP-1 levels. As opposed to IL-6 and MCP-1, YKL-40 is not expressed by neurons or astrocytes. Because YKL-40 was shown to be expressed in late-stage of macrophage differentiation and its CSF concentration is tightly associated with the kinetics of CSF SIV viral load, it could be a more specific marker of meningo-encephalitis associated with CNS SIV infection.

Expression of YKL-40 in the CNS

To study the expression pattern of YKL-40 in the CNS and during encephalitis we first evaluated its expression

in mixed neuronal/glia cultures. We determined that YKL-40 is expressed and secreted by microglia in culture but not astrocytes or neurons. Because macrophages secrete large amounts of YKL-40 *in vitro*, and M-CSF was able to attenuate release, perivascular macrophages are potentially the origin of YKL-40 in the brain and CSF. This was confirmed by *in situ* hybridization showing that YKL-40 mRNA is indeed co-localized with microglia/macrophages in SIVE. We are not aware of previous publications describing the relation between YKL-40 release and HIV infection, however, our unpublished early findings suggest that HIV infection induces YKL-40 release at the beginning of infection. We were surprised to find most of

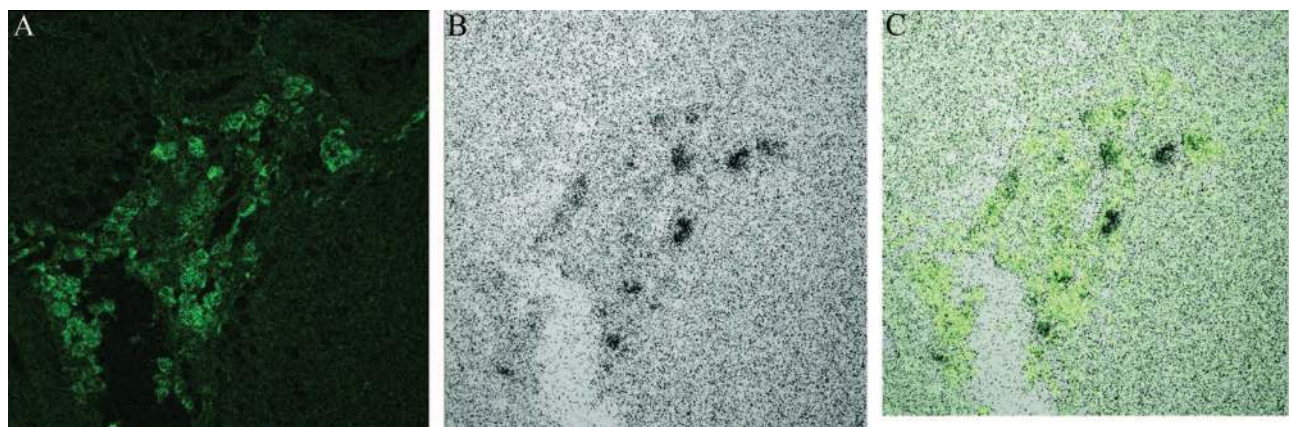


Figure 9. YKL-40 mRNA co-localizes with microglia/macrophages. Six- μ m-thick paraffin-embedded section were stained with CD68 (**A**) and then hybridized with 35 S-labeled RNA probes for YKL-40 (**B**) as described in the Materials and Methods. **C:** Grains predominantly localize with CD68-positive cell bodies.

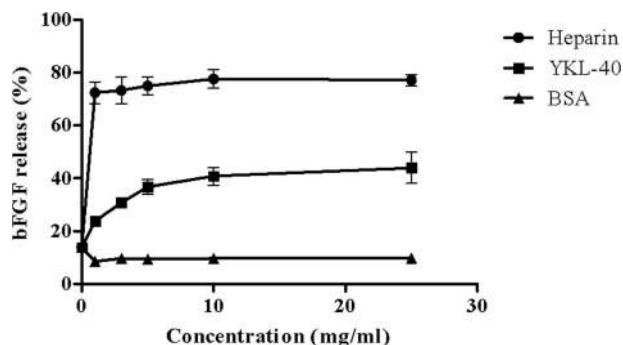


Figure 10. YKL-40 displacement of ECM-bound bFGF. ECM-coated wells were incubated with ^{125}I -bFGF. The ECM was then washed to remove the unbound bFGF, and incubated with increasing concentrations of heparin, bovine serum albumin, or YKL-40. Released ^{125}I -bFGF was counted in a γ -counter. Released radioactivity is expressed as percentage of total ECM-bound ^{125}I -bFGF. Each data point is the mean of duplicate wells (\pm SEM). The results are representative of at least three different experiments.

the YKL-40 immunoreactivity associated around some of activated astrocytes. Roberts and colleagues⁵³ previously reported that YKL-40 mRNA appeared in the white matter in the vicinity of lesions predominately in cells presumed to be astrocytes as determined by *in situ* hybridization for YKL-40. In agreement with the *in vitro* findings YKL-40 mRNA was found associated with microglia/macrophages *in vivo*, however the protein was probably secreted and deposited around or taken up by astrocytes in the vicinity of microglial nodules *in vivo* by an unknown mechanism.

Potential Role of YKL-40 in Neurodegeneration

The finding that YKL-40 levels increased specifically in the CSF suggests that YKL-40 may play a specific role in neurodegeneration associated with SIVE. YKL-40 expression is characteristic of other chronic inflammatory conditions such as rheumatoid arthritis, osteoarthritis, and irritable bowel disorder that are also associated with ECM destruction and tissue remodeling.⁵⁴ It is intriguing to

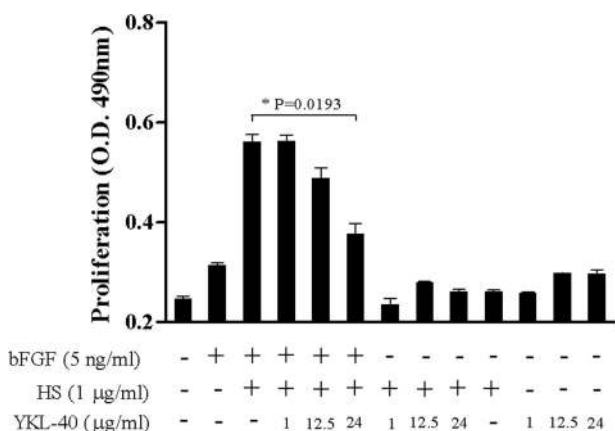


Figure 11. YKL-40 inhibits the mitogenic activity of bFGF in FGFR1-expressing BaF3 cells. Proliferation of FGFR1-expressing cells was evaluated using Promega's CellTiter kit. The cells were incubated with 5 ng/ml of bFGF and the indicated concentrations of heparan sulfate and purified YKL-40. Heparan sulfate and YKL-40 were mixed and incubated on ice for 1 hour before their addition. Each point is the mean value of triplicate samples (\pm SEM). The results are representative of at least three different experiments.

consider that YKL-40 might play a role in the remodeling of the ECM in the brain and accompanying neuronal dysfunction seen in encephalitis.

It is not known if the function of YKL-40 in macrophages is the same as in cancer cells but YKL-40 seems to play an important role in tumor invasiveness and may facilitate macrophage migration through the tissue parenchyma. YKL-40 is elevated in serum of patients with primary or metastatic carcinoma of the breast, colon, lung, prostate, and glioblastoma and is being considered as a prognostic marker of short recurrence and poor prognosis.⁵⁵⁻⁵⁹

Mode of Action of YKL-40

No specific receptor for YKL-40 has been identified. The fact that this is a released protein suggests that it probably acts on the ECM or cells in an autocrine/paracrine manner. Fusetti and colleagues⁵ have showed that YKL-40 contains a putative heparin binding site but heparan sulfate is more likely to bind to YKL-40. In addition it has two potential hyaluronic acid binding motifs. Heparan sulfates and hyaluronic acids are components of the ECM implying that YKL-40's biological activity relates to its ability to bind these molecules. We found that YKL-40 indeed can bind to the ECM secreted from bovine corneal endothelial cells and by doing so can displace ECM-bound bFGF suggesting that both proteins bind to the same or closely related binding sites in the ECM. The ability of growth factors like bFGF, vascular endothelial growth factor, and epidermal growth factor to bind heparan sulfate enables them to bind to the ECM creating a local reservoir of growth factors. This reservoir allows the spatial regulation of growth factor signaling that is regulated by the mobility of the growth factor from this reservoir to a target cell surface receptor. There are currently two known mechanisms for the release of growth factors from the ECM reservoir: enzymatic cleavage by proteases and heparanases or binding to a carrier protein that can then deliver the growth factor to its receptor.^{60,61} In this study YKL-40 exhibits another mechanism by which growth factors such as bFGF can be released from the ECM via displacing from the binding sites. Further studies must be performed to determine the ability of YKL-40 to release other growth factor, cytokines, and chemokines from the ECM.

The ability of YKL-40 to release ECM-bound bFGF from the ECM raises the question of whether YKL-40 could also interfere with the cell surface receptor signaling. The current hypothesis is that in order for FGF to induce cell signaling a ternary complex of FGF, FGFR, and heparan sulfate must form to enable receptor dimerization and subsequent tyrosine phosphorylation. Both FGF and FGFR simultaneously interact with heparan sulfate chains.⁶² YKL-40 inhibited the mitogenic response of bFGF and heparan sulfates in FGFR1-expressing BaF3 cells in a dose-dependent manner. YKL-40 did not compete for the binding of bFGF to FGFR1 in cross-linking experiments (data not shown), therefore it may cause a spatial interference

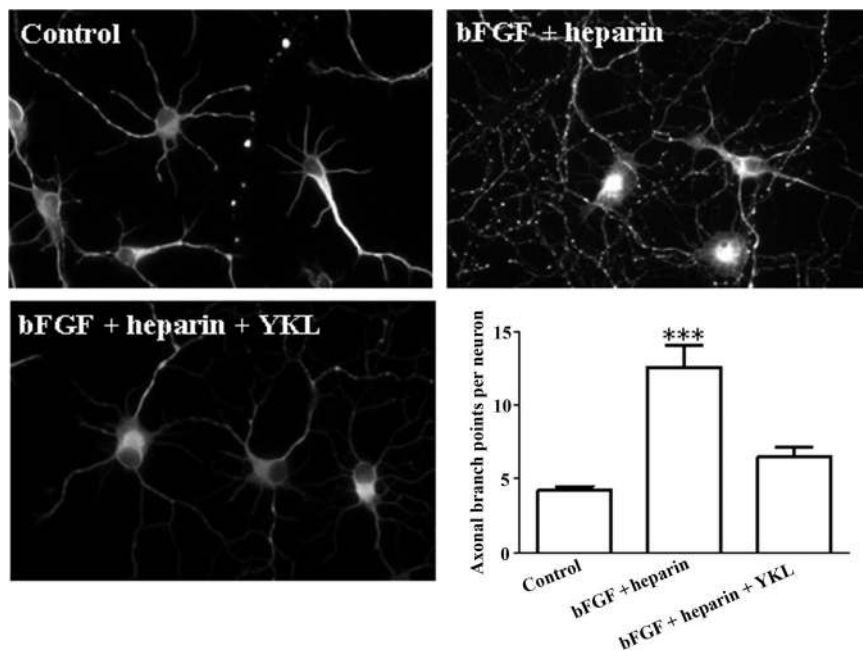


Figure 12. YKL-40 inhibits bFGF-induced axonal branching of hippocampal neurons. Hippocampal cultures were prepared from E18 Sprague-Dawley pregnant rats and plated on coverslips on astrocyte feeder layer for 2 days. After 2 days the coverslips were transferred to a new plate and grown in serum-free N2 medium without the feeder layer for an additional 2 days in the absence or presence of bFGF (10 ng/ml), heparin (1 ng/ml), and YKL (12.5 μ g/ml) as indicated. On day 4 in culture the cells were fixed and labeled with tau. Axonal quantification was done as described in the Materials and Methods. The number of axonal branch points per neuron was counted. A one-way analysis of variance with posthoc comparison via Tukey's honestly significant difference was used to evaluate between group differences.

between the heparan sulfate chains and the formation of the ternary complex but does not interfere with the binding of bFGF to FGFR1. The physiological concentrations of YKL-40 found in purulent meningitis (20 to 8960 ng/ml) and encephalitis (620 to 11,600 ng/ml) in humans and those found in this study (1077 to 2662 ng/ml) are in the range capable of releasing ECM-bound bFGF and inhibiting FGFR1 signaling. It is important to note that the macaques were sacrificed when moribund with AIDS thus YKL-40 could have reached higher levels if we would have taken measures to extend their lives.

The ability of YKL-40 to release ECM-bound bFGF probably would not induce bFGF signaling because it is displaced and not released as a complex of bFGF-heparan sulfate by heparanase or plasmin with less likelihood to diffuse to target cells.^{63,64} Thus the net biological effect of YKL-40 is inhibition of bFGF signaling and potentially other trophic factors. bFGF was shown to be neuroprotective in models of ischemia, excitotoxicity induced by glutamate or kainic acid, and axotomy-induced death. Loss of trophic support has long been considered in neurodegenerative diseases. Various reports show a decrease in BDNF in the hippocampus of individuals with Alzheimer's disease.⁶⁵ BDNF, GDNF, CNTF, and bFGF were shown to be decreased in Parkinson's disease.⁶⁶ Studies performed in animal models showed that NGF infusion reversed age-associated decline in basal forebrain cholinergic neurons in aged rats and nonhuman primate brain.⁶⁷ Therefore YKL-40 could contribute to neuronal loss indirectly by blocking trophic support. YKL-40 by itself did not induce neuronal death in primary cultures but it was able to significantly inhibit bFGF-induced axonal branching. Thus YKL-40 potentially has the capacity to induce changes in the functionality of the neurons or plasticity induced by growth

factors.⁶⁸⁻⁷⁰ Further studies are required to determine the role of YKL-40 in neurodegeneration.

In summary, our data demonstrate that increased YKL-40 release by microglia/macrophages in SIV encephalitis can serve as a CSF biomarker for SIV encephalitis. Further, the *in vivo* distribution of YKL-40 around the soma of reactive astrocytes and the *in vitro* capacity of YKL-40 to displace bFGF imply an important role for this molecule in the pathogenesis of HIV encephalitis. Beyond secretion of cytokines, chemokines, and degradative enzymes, microglia/macrophages can also interact with the ECM through molecules such as YKL-40 to release growth factors from their ECM reservoir and thus modulate growth factor activity potentially leading to neurodegeneration.

Acknowledgments

We thank Dawn McClemens-McBride for organizing all of the animal procedures; Professor David M. Ornitz for providing us with the FGFR1-expressing BaF3 cells; Jason Nguyen, Adam Starkey, Amy L. Sartori, and Nnaja Okorafor for valuable technical support; Dr. Geoffrey Murdoch for valuable discussion; Dr. Todd Rheinart for *in situ* hybridization methodology; and the National NeuroAIDS Tissue Consortium for providing human CSF samples.

References

1. Navia BA, Jordan BD, Price RW: The AIDS dementia complex: I. Clinical features. *Ann Neurol* 1986, 19:517-524
2. Wiley CA, Achim C: Human immunodeficiency virus encephalitis is the pathological correlate of dementia in acquired immunodeficiency syndrome. *Ann Neurol* 1994, 36:673-676
3. Everall I, Luthert P, Lantos P: A review of neuronal damage in human

- immunodeficiency virus infection: its assessment, possible mechanism and relationship to dementia. *J Neuropathol Exp Neurol* 1993, 52:561–566
4. Medina-Flores R, Wang G, Bissel SJ, Murphey-Corb M, Wiley CA: Destruction of extracellular matrix proteoglycans is pervasive in simian retroviral neuroinfection. *Neurobiol Dis* 2004, 16:604–616
 5. Fusetti F, Pijning T, Kalk KH, Bos E, Dijkstra BW: Crystal structure and carbohydrate-binding properties of the human cartilage glycoprotein-39. *J Biol Chem* 2003, 278:37753–37760
 6. Bigg HF, Wait R, Rowan AD, Cawston TE: The mammalian chitinase-like lectin, YKL-40, binds specifically to type I collagen and modulates the rate of type I collagen fibril formation. *J Biol Chem* 2006, 281:21082–21095
 7. Kirkpatrick RB, Emery JG, Connor JR, Dodds R, Lysko PG, Rosenberg M: Induction and expression of human cartilage glycoprotein 39 in rheumatoid inflammatory and peripheral blood monocyte-derived macrophages. *Exp Cell Res* 1997, 237:46–54
 8. Rehli M, Nillner HH, Ammon C, Langmann S, Schwarzfischer L, Andreessen R, Krause SW: Transcriptional regulation of CHI3L1, a marker gene for late stages of macrophage differentiation. *J Biol Chem* 2003, 278:44058–44067
 9. Recklies AD, White C, Ling H: The chitinase 3-like protein human cartilage glycoprotein 39 (HC-gp39) stimulates proliferation of human connective-tissue cells and activates both extracellular signal-regulated kinase- and protein kinase B-mediated signalling pathways. *Biochem J* 2002, 365:119–126
 10. Recklies AD, Ling H, White C, Bernier SM: Inflammatory cytokines induce production of CHI3L1 by articular chondrocytes. *J Biol Chem* 2005, 280:41213–41221
 11. Ling H, Recklies AD: The chitinase 3-like protein human cartilage glycoprotein 39 inhibits cellular responses to the inflammatory cytokines interleukin-1 and tumour necrosis factor- α . *Biochem J* 2004, 380:651–659
 12. Nishikawa KC, Millis AJ: gp38k (CHI3L1) is a novel adhesion and migration factor for vascular cells. *Exp Cell Res* 2003, 287:79–87
 13. Zhang JY, Martin LN, Watson EA, Montelaro RC, West M, Epstein L, Murphey-Corb M: Simian immunodeficiency virus/delta-induced immunodeficiency disease in rhesus monkeys: relation of antibody response and antigenemia. *J Infect Dis* 1988, 158:1277–1286
 14. Bissel SJ, Wang G, Ghosh M, Reinhart TA, Capuano III S, Stefano Cole K, Murphey-Corb M, Piatak M Jr, Lifson JD, Wiley CA: Macrophages relate presynaptic and postsynaptic damage in simian immunodeficiency virus encephalitis. *Am J Pathol* 2002, 160:927–941
 15. Fuller DH, Rajakumar PA, Wilson LA, Trichel AM, Fuller JT, Shipley T, Wu MS, Weis K, Rinaldo CR, Haynes JR, Murphey-Corb M: Induction of mucosal protection against primary, heterologous simian immunodeficiency virus by a DNA vaccine. *J Virol* 2002, 76:3309–3317
 16. Wiley CA, Soontornniyomkij V, Radhakrishnan L, Maslah E, Mellors J, Hermann SA, Dailey P, Achim CL: Distribution of brain HIV load in AIDS. *Brain Pathol* 1998, 8:277–284
 17. Zhu JH, Kulich SM, Oury TD, Chu CT: Cytoplasmic aggregates of phosphorylated extracellular signal-regulated protein kinases in Lewy body diseases. *Am J Pathol* 2002, 161:2087–2098
 18. Repnik U, Knezevic M, Jeras M: Simple and cost-effective isolation of monocytes from buffy coats. *J Immunol Methods* 2003, 278:283–292
 19. Barami K, Grever WE, Diaz FG, Lyman WD: An efficient method for the culturing and generation of neurons and astrocytes from second trimester human central nervous system tissue. *Neurol Res* 2001, 23:321–326
 20. Aridor M, Guzik AK, Bielli A, Fish KN: Endoplasmic reticulum export site formation and function in dendrites. *J Neurosci* 2004, 24:3770–3776
 21. Reinhart TA, Fallert BA, Pfeifer ME, Sanghavi S, Capuano S III, Rajakumar P, Murphey-Corb M, Day R, Fuller CL, Schaefer TM: Increased expression of the inflammatory chemokine CXC chemokine ligand 9/monokine induced by interferon- γ in lymphoid tissues of rhesus macaques during simian immunodeficiency virus infection and acquired immunodeficiency syndrome. *Blood* 2002, 99:3119–3128
 22. Benezra M, Ishai-Michaeli R, Ben-Sasson SA, Vlodavsky I: Structure-activity relationships of heparin-mimicking compounds in induction of bFGF release from extracellular matrix and inhibition of smooth muscle cell proliferation and heparanase activity. *J Cell Physiol* 2002, 192:276–285
 23. Ornitz DM, Yayon A, Flanagan JG, Svahn CM, Levi E, Leder P: Heparin is required for cell-free binding of basic fibroblast growth factor to a soluble receptor and for mitogenesis in whole cells. *Mol Cell Biol* 1992, 12:240–247
 24. Zhang X, Ibrahim OA, Olsen SK, Umemori H, Mohammadi M, Ornitz DM: Receptor specificity of the fibroblast growth factor family. The complete mammalian FGF family. *J Biol Chem* 2006, 281:15694–15700
 25. Ranganathan S, Williams E, Ganchev P, Gopalakrishnan V, Lacomis D, Urbinelli L, Newhall K, Cudkowicz ME, Brown RH Jr, Bowser R: Proteomic profiling of cerebrospinal fluid identifies biomarkers for amyotrophic lateral sclerosis. *J Neurochem* 2005, 95:1461–1471
 26. Dumont D, Noben JP, Raus J, Stinissen P, Robben J: Proteomic analysis of cerebrospinal fluid from multiple sclerosis patients. *Proteomics* 2004, 4:2117–2124
 27. Choe LH, Dutt MJ, Relkin N, Lee KH: Studies of potential cerebrospinal fluid molecular markers for Alzheimer's disease. *Electrophoresis* 2002, 23:2247–2251
 28. Davidsson P, Sjogren M, Andreassen N, Lindbjerg M, Nilsson CL, Westman-Brinkmalm A, Blennow K: Studies of the pathophysiological mechanisms in frontotemporal dementia by proteome analysis of CSF proteins. *Brain Res Mol Brain Res* 2002, 109:128–133
 29. Tsuji T, Shiozaki A, Kohno R, Yoshizato K, Shimohama S: Proteomic profiling and neurodegeneration in Alzheimer's disease. *Neurochem Res* 2002, 27:1245–1253
 30. Zheng PP, Luider TM, Pieters R, Avezaat CJ, van den Bent MJ, Sillevis Smitt PA, Kros JM: Identification of tumor-related proteins by proteomic analysis of cerebrospinal fluid from patients with primary brain tumors. *J Neuropathol Exp Neurol* 2003, 62:855–862
 31. Luo X, Carlson KA, Wojna V, Mayo R, Biskup TM, Stoner J, Anderson J, Gendelman HE, Melendez LM: Macrophage proteomic fingerprinting predicts HIV-1-associated cognitive impairment. *Neurology* 2003, 60:1931–1937
 32. Wojna V, Carlson KA, Luo X, Mayo R, Melendez LM, Kraiselburd E, Gendelman HE: Proteomic fingerprinting of human immunodeficiency virus type 1-associated dementia from patient monocyte-derived macrophages: a case study. *J Neurovirol* 2004, 10(Suppl 1):S74–S81
 33. Berger JR, Avison M, Mootoor Y, Beach C: Cerebrospinal fluid proteomics and human immunodeficiency virus dementia: preliminary observations. *J Neurovirol* 2005, 11:557–562
 34. Kronborg G, Ostergaard C, Weis N, Nielsen H, Obel N, Pedersen SS, Price PA, Johansen JS: Serum level of YKL-40 is elevated in patients with *Streptococcus pneumoniae* bacteremia and is associated with the outcome of the disease. *Scand J Infect Dis* 2002, 34:323–326
 35. Østergaard C, Johansen JS, Benfield T, Price PA, Lundgren JD: YKL-40 is elevated in cerebrospinal fluid from patients with purulent meningitis. *Clin Diagn Lab Immunol* 2002, 9:598–604
 36. Johansen JS: Studies on serum YKL-40 as a biomarker in diseases with inflammation, tissue remodelling, fibroses and cancer. *Dan Med Bull* 2006, 53:172–209
 37. Powers CJ, McLeskey SW, Wellstein A: Fibroblast growth factors, their receptors and signaling. *Endocr Relat Cancer* 2000, 7:165–197
 38. Vaday GG, Lider O: Extracellular matrix moieties, cytokines, and enzymes: dynamic effects on immune cell behavior and inflammation. *J Leukoc Biol* 2000, 67:149–159
 39. Szebenyi G, Dent EW, Callaway JL, Seys C, Lueth H, Kalil K: Fibroblast growth factor-2 promotes axon branching of cortical neurons by influencing morphology and behavior of the primary growth cone. *J Neurosci* 2001, 21:3932–3941
 40. Katsuki H, Itsukaichi Y, Matsuki N: Distinct signaling pathways involved in multiple effects of basic fibroblast growth factor on cultured rat hippocampal neurons. *Brain Res* 2000, 885:240–250
 41. Morrison RS, Sharma A, de Vellis J, Bradshaw RA: Basic fibroblast growth factor supports the survival of cerebral cortical neurons in primary culture. *Proc Natl Acad Sci USA* 1986, 83:7537–7541
 42. Ferrari G, Minozzi MC, Toffano G, Leon A, Skaper SD: Basic fibroblast growth factor promotes the survival and development of mesencephalic neurons in culture. *Dev Biol* 1989, 133:140–147
 43. Walicke P, Cowan WM, Ueno N, Baird A, Guillemin R: Fibroblast growth factor promotes survival of dissociated hippocampal neurons and enhances neurite extension. *Proc Natl Acad Sci USA* 1986, 83:3012–3016
 44. Hatten ME, Lynch M, Rydel RE, Sanchez J, Joseph-Silverstein J, Moscatelli D, Rifkin DB: In vitro neurite extension by granule neurons

- is dependent upon astroglial-derived fibroblast growth factor. *Dev Biol* 1988, 125:280–289
45. Zink MC, Suryanarayana K, Mankowski JL, Shen A, Piatak M Jr, Spelman JP, Carter DL, Adams RJ, Lifson JD, Clements JE: High viral load in the cerebrospinal fluid and brain correlates with severity of simian immunodeficiency virus encephalitis. *J Virol* 1999, 73:10480–10488
 46. Bissel SJ, Wang G, Trichel AM, Murphey-Corb M, Wiley CA: Longitudinal analysis of monocyte/macrophage infection in simian immunodeficiency virus-infected, CD8+ T-cell-depleted macaques that develop lentiviral encephalitis. *Am J Pathol* 2006, 168:1553–1569
 47. Cinque P, Vago L, Ceresa D, Mainini F, Terreni MR, Vagani A, Torri W, Bossolasco S, Lazzarin A: Cerebrospinal fluid HIV-1 RNA levels: correlation with HIV encephalitis. *AIDS* 1998, 12:389–394
 48. Helke KL, Queen SE, Tarwater PM, Turchan-Cholewo J, Nath A, Zink MC, Irani DN, Mankowski JL: 14-3-3 protein in CSF: an early predictor of SIV CNS disease. *J Neuroopathol Exp Neurol* 2005, 64:202–208
 49. Towfighi A, Skolasky RL, St Hillaire C, Conant K, McArthur JC: CSF soluble Fas correlates with the severity of HIV-associated dementia. *Neurology* 2004, 62:654–656
 50. Gelbard HA, Nottet HS, Swindells S, Jett M, Dzenko KA, Genis P, White R, Wang L, Choi YB, Zhang D, Lipton SA, Tourtellotte WW, Epstein LG, Gendelman HE: Platelet-activating factor: a candidate human immunodeficiency virus type 1-induced neurotoxin. *J Virol* 1994, 68:4628–4635
 51. Foldi M, Castagna A, Parma M, Piona A, Tedeschi A, Miadonna A, Lorini M, Orazio EN, Lazzarin A: Mediator release in cerebrospinal fluid of human immunodeficiency virus-positive patients with central nervous system involvement. *J Neuroimmunol* 1992, 38:155–161
 52. Heyes MP, Saito K, Lackner A, Wiley CA, Achim CL, Markey SP: Sources of the neurotoxin quinolinic acid in the brain of HIV-1-infected patients and retrovirus-infected macaques. *FASEB J* 1998, 12:881–896
 53. Roberts ES, Zandonatti MA, Watry DD, Madden LJ, Henriksen SJ, Taffe MA, Fox HS: Induction of pathogenic sets of genes in macrophages and neurons in NeuroAIDS. *Am J Pathol* 2003, 162:2041–2057
 54. Rathcke CN, Vestergaard H: YKL-40, a new inflammatory marker with relation to insulin resistance and with a role in endothelial dysfunction and atherosclerosis. *Inflamm Res* 2006, 55:221–227
 55. Jensen BV, Johansen JS, Price PA: High levels of serum HER-2/neu and YKL-40 independently reflect aggressiveness of metastatic breast cancer. *Clin Cancer Res* 2003, 9:4423–4434
 56. Cintin C, Johansen JS, Christensen IJ, Price PA, Sorensen S, Nielsen HJ: Serum YKL-40 and colorectal cancer. *Br J Cancer* 1999, 79:1494–1499
 57. Johansen JS, Drivsholm L, Price PA, Christensen IJ: High serum YKL-40 level in patients with small cell lung cancer is related to early death. *Lung Cancer* 2004, 46:333–340
 58. Brasso K, Christensen IJ, Johansen JS, Teisner B, Garner P, Price PA, Iversen P: Prognostic value of PINP, bone alkaline phosphatase, CTX-I, and YKL-40 in patients with metastatic prostate carcinoma. *Prostate* 2006, 66:503–513
 59. Hormigo A, Gu B, Karimi S, Riedel E, Panageas KS, Edgar MA, Tanwar MK, Rao JS, Fleisher M, DeAngelis LM, Holland EC: YKL-40 and matrix metalloproteinase-9 as potential serum biomarkers for patients with high-grade gliomas. *Clin Cancer Res* 2006, 12:5698–5704
 60. Aigner A, Butscheid M, Kunkel P, Krause E, Lamszus K, Wellstein A, Czubyko F: An FGF-binding protein (FGF-BP) exerts its biological function by parallel paracrine stimulation of tumor cell and endothelial cell proliferation through FGF-2 release. *Int J Cancer* 2001, 92:510–517
 61. Vlodavsky I, Korner G, Ishai-Michaeli R, Bashkin P, Bar-Shavit R, Fuks Z: Extracellular matrix-resident growth factors and enzymes: possible involvement in tumor metastasis and angiogenesis. *Cancer Metastasis Rev* 1990, 9:203–226
 62. Wu ZL, Zhang L, Yabe T, Kuberan B, Beeler DL, Love A, Rosenberg RD: The involvement of heparan sulfate (HS) in FGF1/HS/FGFR1 signaling complex. *J Biol Chem* 2003, 278:17121–17129
 63. Rifkin DB, Moscatelli D: Recent developments in the cell biology of basic fibroblast growth factor. *J Cell Biol* 1989, 109:1–6
 64. Ishai-Michaeli R, Eldor A, Vlodavsky I: Heparanase activity expressed by platelets, neutrophils, and lymphoma cells releases active fibroblast growth factor from extracellular matrix. *Cell Regul* 1990, 1:833–842
 65. Phillips HS, Hains JM, Armanini M, Laramée GR, Johnson SA, Winslow JW: BDNF mRNA is decreased in the hippocampus of individuals with Alzheimer's disease. *Neuron* 1991, 7:695–702
 66. Siegel GJ, Chauhan NB: Neurotrophic factors in Alzheimer's and Parkinson's disease brain. *Brain Res Brain Res Rev* 2000, 33:199–227
 67. Fischer W, Victorin K, Bjorklund A, Williams LR, Varon S, Gage FH: Amelioration of cholinergic neuron atrophy and spatial memory impairment in aged rats by nerve growth factor. *Nature* 1987, 329:65–68
 68. Bethel A, Kirsch JR, Koehler RC, Finklestein SP, Traystman RJ: Intravenous basic fibroblast growth factor decreases brain injury resulting from focal ischemia in cats. *Stroke* 1997, 28:606–615
 69. Guo Q, Sebastian L, Sopher BL, Miller MW, Glazner GW, Ware CB, Martin GM, Mattson MP: Neurotrophic factors [activity-dependent neurotrophic factor (ADNF) and basic fibroblast growth factor (bFGF)] interrupt excitotoxic neurodegenerative cascades promoted by a PS1 mutation. *Proc Natl Acad Sci USA* 1999, 96:4125–4130
 70. Tretter YP, Hertel M, Munz B, ten Bruggencate G, Werner S, Alzheimer C: Induction of activin A is essential for the neuroprotective action of basic fibroblast growth factor in vivo. *Nat Med* 2000, 6:812–815